EXPERIMENTAL AND NUMERICAL STUDIES ON VIBRATIONS OF BUILDINGS

by

Hatsuo ISHIZAKI* and Naotaka HATAKEYAMA**

1. Introduction

As the fundamental problems for aseismic design of buildings, what vibration characteristics the buildings have or especially the special parts of them have and what influences to the vibrations of buildings the ground has, are taken up in this paper. They were studied by the experiments on buildings and some advices for the aseismic design of buildings are derived.

By the experiments, we could not see the vibration character out of the elastic range so that the elastic-plastic vibrations due to shearing deformations have been treated by numerical computations. In discussions of each paragraph, the distributions of lateral force coefficients, the ground effect for earthquake forces and the vibration behavior in the plastic range are reviewed.

2. Vibration tests of buildings

(i) Deformations of the floor of a building

In vibration tests of many buildings, the horizontal displacement distributions or deformations together with the periods in vertical direction have been observed, but in the horizontal direction, a few experiments have been made until today. Here we have experimented a building with the purpose to study the displacement or amplitude distributions in the horizontal direction and the deformations of floors.

As shown in Fig.1, a four-storied reinforced concrete building having a simple rectangular plan, was tested and since it was near the railway, the vibrations caused by trains were observed. The instruments used were moving coil

---

* Prof. of Disaster Prevention Research Inst.,Kyoto Univ.
** Asst. Prof. of Civ. Eng., Ritsumeikan Univ.

type vibrographs having the natural frequency of 2 cycles per second and an electro-magnetic oscillograph recorder with galvanometers having the natural frequency of 15 cycles per second. The characteristics of vibrographs were already reported by Dr.M.Hatanaka[5].

An example of horizontal displacement distributions in the vertical direction is shown in Fig.2. Three typical displacement distributions in the horizontal direction are shown in Figs.3, 4 and 5, the periods corresponding to each distribution are noted in the figures and the dotted lines in them are sine curves. The curve in Fig.3 corresponds to the first mode of vibration in the horizontal direction, the curve in Fig.4 has one node and is fit for the second mode and the curve in Fig.5 is the third mode.

In the case of Fig.3, the building was a little twisted but the case of Fig.4 shows so-called a torsional vibration and the case of Fig.5 is double twisted vibration. As the vibration of the last type will occur also in violent earthquakes, it is not sufficient for aseismic design considering a simple torsional vibration alone such as in this building. We must take into account the deformations due to the higher modes of vibrations of buildings in the horizontal direction.

(ii) Vibrations of the tower of a building

The amplitudes of towers on buildings or penthouses during vibrations will be greater than the amplitudes of buildings below, but how much greater they are, is not yet specified. We have observed the vibrations of the tower of Kyoto Station shown in Fig.6, and compared the amplitude distribution with that of the building below.

The experiments were made in the same manner as illustrated in the previous section, and as the result, the obtained amplitude or displacement distributions are shown in Fig.7. The observed displacement are approximately on the sine curves in the figures. From the figures, we can see that in elastic range the lateral force coefficient for the tower must be at least two times greater than the coefficient for the building below.

(iii) Vibrations of under ground parts of a building

The vibrations of a building shown in Fig.8, of 12 stories above and 3 stories under ground, were observed in the same manner as above. The natural periods obtained are in the N-S direction: 0.55, 0.51, 0.47, 0.40, 0.27, 0.11 sec, in the E-W direction: 0.50, 0.46, 0.41, 0.35, 0.12 sec. The distributions of horizontal displacements in the vertical direction are shown by the points in Fig.9. Why these distributions occured, will be considered in the following.

Taking the shearing deformations of building alone into account, the equations of vibrations are

for the part under ground $$AG\frac{\partial^2 u_i}{\partial x_i^2} + k b u_i = A\rho\frac{\partial^2 u_i}{\partial t^2} \qquad (1)$$

for the part above ground $$G\frac{\partial^2 u_2}{\partial x^2}=\rho\frac{\partial^2 u_2}{\partial t^2} \qquad (2)$$

Where
A : cross-section area of the building
G : modulus of rigidity " "
ρ : average density " "
u_1, u_2 : displacement " "
b : width of the building in the direction perpendicular to the displacement
k : coefficient of subgrade reaction

If we put

$$u_1 = U_1(x_1)e^{int}, \quad u_2 = U_2(x_2)e^{int},$$

the boundary conditions

$$x_1=0;\ \frac{dU_1}{dx_1}=cU_1, \qquad x_2=l_2;\ \frac{dU_2}{dx_2}=0,$$

and the conditions of continuity

$$x_1=l_1,\ x_2=0;\ U_1=U_2,\ \frac{dU_1}{dx_1}=\frac{dU_2}{dx_2},$$

the solutions of free vibrations are written as

$$\left.\begin{aligned} U_1 &= C\left(\sin\alpha x_1+\frac{\alpha}{c}\cos\alpha x_1\right)\\ U_2 &= C\left(\cos\alpha l_1-\frac{\alpha}{c}\sin\alpha l_1\right)\frac{\alpha}{\beta}\left(\sin\beta x_1+\cos\beta l_2\cos\beta x_2\right),\end{aligned}\right\} \qquad (3)$$

where

$$\alpha^2=\frac{kb}{AG}+\frac{\rho}{G}n^2, \quad \beta^2=\frac{\rho}{G}n^2. \qquad (4)$$

The frequency equation is

$$\alpha l_1\frac{cl_1-\alpha l_1\tan\alpha l_1}{\alpha l_1+cl_1\tan\alpha l_1}=\beta l_1\tan\beta l_2. \qquad (5)$$

Putting the dimensions of the building

$$l_1=9.9^m,\ l_2=41^m,\ A=2000^{m^2},\ b=41^m,$$

and the assumed values

$$k=6\ ^{kg}/_{cm^3}, \qquad cl_1=5$$

into the above equations, we can get each mode of free vibration shown in Fig.10 and the ratio of periods corresponding to the first, second and third modes, is as follows.

$$T_1 : T_2 : T_3 = 1.00 : 0.336 : 0.207$$

When the fundamental periods are 0.55 sec and 0.50 sec in each direction, the periods of the second and third modes are computed from above ratio.

T_1	T_2	T_3	
0.55	0.18	0.11	sec
0.50	0.17	0.10	sec

The periods obtained by the experiment, which are different from the above values, are perhaps due to the torsional vibrations of the deformation of floors.

The curves in Fig.9 are obtained by combining the modes shown in Fig.10 that were calculated by the equations (3). The points in the figure got from the records, lie almost on the calculated curves. We can conclude here that the above elementary analysis explains the results of experiments for the building having the under ground part, and the lateral force coefficients for it might be taken as smaller values, because the deformations of structures in the ground will be small even in violent earthquakes.

3. Effects of grounds to vibrations of reinforced concrete buildings

The earthquake forces against structures are apparently influenced by the ground where they stand and one of the authors have discussed the relations between the earthquake damages of wooden structures and the ground properties.[2] But how the earthquake forces against reinforced concrete buildings will be effected by the ground, has not yet answered. With the purpose to make clear this problem, we have experimented the vibrations of reinforced concrete buildings having the same type and dimensions of frames but located on different grounds. The buildings experimented are schools shown in Fig. 11 and their situations are shown in Fig.12.

(i) Vibrations caused by the micro-tremors of grounds

The behaviors of micro-tremors are different from the waves of earthquakes, but it is well known that their characteristics show some of the ground properties. We have set the vibrographs on the buildings floors and on the ground surface and the vibrations by ordinary micro-tremors were measured.

(1) Measurements of vibrations. The vibrographs used were moving coil type as above and equipped situations are shown in Fig.13. They were connected to an electromagnetic oscillograph recorder. Some of the records obtained are shown in Fig.14 and the curves in the figure shown irregular patterns of vibration, so we have determined the periods of them conveniently as follows. At first, a straight line was drawn through the midpoint of the amplitude shown by the curves in the records, and twice of time intervals between the neighbouring points where the line intersects the curve in the record was assumed as the period. The period numbers obtained in this way from the records were summed up in every time difference 0.02 sec and they were defined as the frequency distributions of periods. (cf.Table 1)

(2) Consideration. As seen from Fig.14, the vibrations of the buildings have longer periods in spite of that the considerable shorter periods appear on the grounds. As shown in Fig.15, the predominating periods of buildings are longer than that of the grounds. The curves of frequency distributions can be divided into three groups, (A), (B) and (C). Group (A) is the type having a distinct peak, (B) is the type having two peaks and (C) is a flat curve without any distinct peaks.

The relation between the predominant periods of buildings and that of grounds is shown in Fig.16. The former becomes longer together with the latter. The relation between the periods of buildings and the thickness of alluvium layers in Fig.17 is not distinct.

The ratio of wave numbers having the predominant periods to the numbers of all waves will be called the probability of predominant periods. The relation between the periods of buildings and the probability is shown in Fig.18 and from the figure, we can see that the probability becomes larger as the periods becomes shorter. The tendency appears alsc in that of grounds. The relation between the periods ratio of buildings to grounds and the periods of grounds is shown in Fig.19. The period ratio becomes larger as the period becomes shorter. This is originated in the fact that in the case as the ground has shorter periods, the difference between the periods of ground and proper natural periods of buildings without the ground effects will be large, because the periods of ground are about 0.08 - 0.20 sec and the periods of buildings are more than 0.20 sec. However, in violent earthquakes, the periods of every ground motion will become more longer and the buildings on the ground having shorter periods of micro-tremors will be attacked by stronger forces than the building on the ground having longer periods. Generally, the ground having shorter periods is thought to be good or hard, but for the reinforced concrete buildings, it may be not advantageous, since the periods of earthquake motion grow up near to the natural periods of buildings.

(ii) Free vibration tests of reinforced concrete buildings

The school buildings tested have same structures as above and they are pulled by a wire rope in the horizontal direction and suddenly relaxed. The free vibrations with damping caused in this way were measured to study the influences of grounds to the buildings.

(1) Measurements of vibrations. The buildings tested are Fuku, Obiraki, Himesato and Imamiya Primary Schools in Fig.12. The instruments used were Ishimoto type horizontal vibrograph, 9 moving coil type vibrograph and an oscillograph recorder as above. The horizontal vibrographs were set on the every floor at the center of the buildings in width. The two vertical vibrographs were set at the both ends of width.

An example of the records obtained by the moving coil type vibrographs is shown in Fig.20 and it indicates that the free vibration of a building after being relaxed from the wire rope pulled by a winch. A pretty large amplitude, appeared about the third wave, was caused by the wire rope striking the building.

The displacement distributions of the buildings obtained from the amplitudes in the records, are presented in Figs.21,

22, 23 and 24. These displacements are average values of the experiments executed 4 - 8 times.

As shown in the figures, the horizontal displacements of the floors distribute on a straight line and this line passes near the center of the base floor, or the horizontal displacements on the base is little. The inclination of the base floor was derived from the vertical displacements at the both ends of the floor. The displacements due to the rotation of the building were estimated by the difference between the straight line perpendicular to the inclination line and the original center line of the building. The difference between these displacements and the total displacements in the records were considered to be the elastic deformations. They are shown in the figures and in Table 2. The elastic deformations are about 26 - 36% and the diplacements due to the rotation are about 74 - 64% of the total displacements. The periods obtained from the records are shown in Table 3.

(2) Consideration. The displacements u at the top of the building due to the elastic deformations and the displacements r due to the rotation, are statically

$$u=\frac{Pl}{GA}, \qquad r=\theta l=\frac{Pl^2}{kI}=\frac{12Pl^2}{kAb^2}. \tag{6}$$

Where
- P : force through the wire rope applied the building
- l : height of the building
- θ : rotation at the base " " "
- G : modulus of rigidity " " "
- A : cross-section area " " "
- I : geometrical moment of inertia " " "
- b : width " " "
- k : coefficient of subgrade reaction due to the rotation of the building

Constants, G and k, calculated from the results of the experiments in Table 2, are shown in Table 4. The values of are near to the value 1569 kg/cm² which is calculated from the statical rigidity of walls.

As the total displacements of buildings w are consist of the displacements due to the deformations and the rotations,

$$w(x,t)=u(x,t)+r(x,t).$$

The kinetic energy T, the potential energy V and the damping energy F of the building are

$$\begin{aligned} T &= \frac{\rho A}{2}\int_0^l\left(\frac{\partial w}{\partial t}\right)^2 dx \\ V &= \frac{GA}{2}\int_0^l\left(\frac{\partial u}{\partial x}\right)^2 dx + b'k\int_0^{\frac{b}{2}}(y\theta)\,dy \\ F &= \frac{C_0 A}{2}\int_0^l\left(\frac{\partial u}{\partial t}\right)^2 dx + \frac{C_1 A}{2}\left(\frac{d\theta}{dt}\right)^2 \end{aligned} \tag{7}$$

Where y is horizontal coordinate, b' is length of the building

and C_0 , C_1 are the damping coefficients in the shearing deformations and the ground surface deformation caused by the rotations of the building. Applying the horizontal force to the building at the top, we have the displacements

$$w = \overline{w}\tau = \overline{u}\tau + \overline{r}\tau, \qquad \overline{w} = \frac{P}{GA}x + \frac{Pl}{kI}x = \overline{u} + \overline{r}$$

Then

$$T = \frac{\rho P^2 l^3}{2A}\left(\frac{1}{3G^2} + \frac{8l}{kGb^2} + \frac{48l^2}{k^2b^4}\right)\dot{\tau}^2 = \lambda\dot{\tau}^2$$

$$V = \frac{P^2 l}{2A}\left(\frac{1}{G} + \frac{12l}{kb^2}\right)\tau^2 = \mu\tau^2$$

$$F = \frac{P^2 l^2}{2A}\left(\frac{C_0 l}{3G} + \frac{144C_1}{k^2b^4}\right)\dot{\tau}^2 = \nu\dot{\tau}^2.$$

Substituting these equations into Lagrange's equation

$$\frac{d}{dt}\left(\frac{\partial T}{\partial \dot{\tau}}\right) - \frac{\partial T}{\partial \tau} + \frac{\partial V}{\partial \tau} + \frac{\partial F}{\partial \dot{\tau}} = 0,$$

we can get the following equation

$$\ddot{\tau} + 2\varepsilon\dot{\tau} + n^2\tau = 0, \qquad \varepsilon = \frac{\nu}{2\lambda}, \quad n^2 = \frac{\mu}{\lambda}. \tag{8}$$

The periods of free vibration is

$$T = \frac{2\pi}{\sqrt{n^2 - \varepsilon^2}}, \qquad n^2 = \frac{\frac{C_0 l}{3G} + \frac{144C_1}{k^2b^4}}{2\rho\left(\frac{l}{3G} + \frac{8l^2}{kGb^2} + \frac{48l^4}{k^2b^4}\right)}. \tag{9}$$

If ε^2 is negligible in comparison to n^2,

$$T = 2\pi/n. \tag{10}$$

The average weight of unit volume of the buildings is about 300 kg/m³. If we substitute this value together with the modulus of rigidity and the coefficient of subgrade reaction shown in Table 4, into above equations, the computed periods can be obtained. They are about half of the periods obtained directly from the vibration records. This discrepancy is originated in that we have not taken the energy dissipating into account, in other words, we must consider the vibrations of the buildings together with the surrounding grounds.

The relations between the periods and the velocities of longitudinal, transverse and surface waves in the ground caused by the falling mass, are shown in Figs.25. In these figures, the travelling times of elastic waves in grounds relate almost linearly to the periods of buildings.

4. Vibrations of buildings in plastic range

Aseismic performance of buildings should be considered not only in elastic but also in plastic range of structures, and through the experiments, it is difficult to study the vibration behaviors in plastic range. Although nowadays many contributions on the vibration of plastic systems have been published, in most of them, the buildings treated as one or a few masses. Here we have considered as a continuous body and applied the numerical method to analyse the

vibration.

(i) Finite difference equations of the shearing vibration

As well known the difference equation of shearing vibration of the building having the uniform cross section in the direction of height,

$$\frac{\partial^2 u}{\partial t^2} = \frac{\partial}{\partial x}\left(c\frac{\partial u}{\partial x}\right), \qquad c = \frac{G}{\rho} \ , \tag{11}$$

where $c = f(x)$

or the equation (11) can be written as

$$\frac{\partial^2 u}{\partial t^2} = \frac{\partial c}{\partial x}\frac{\partial u}{\partial x} + c\frac{\partial^2 u}{\partial x^2} . \tag{12}$$

The relation between the stress and train was assumed as the curve shown in Fig.26, which has been generally used for the problems of this kind. In the figure, the line OA shows complete elasticity and AB shows complete plasticity.

The finite difference equation derived from the equation (12) by considering the point pattern illustrated in Fig.27 is

$$u_1 + u_{\mathrm{I}} - 2u_0 = \frac{\tau^2}{h^2}\left[\frac{1}{4}(c_1 - c_2)(u_1 - u_2) + c_2(u_1 + u_2 - 2u_0)\right] \tag{13}$$

In the complete plastic range AB in Fig.26, τ_k is constant and

$$\tau_k = \frac{\alpha}{2h}G = \frac{\chi}{2h}G', \qquad \frac{G'}{\rho} = \frac{\alpha}{\chi}\frac{G}{\rho}$$

or if we put $C_n = G'/\rho$, then $C_n = \frac{\alpha}{\chi}C$. (14)

According to the points 1, 0 and 2 in the figure, are in elastic or plastic range, the following eight equations can be derived.

(I) $c_0 = c_1 = c_2 = c$; $\quad u_{\mathrm{I}} = \frac{\tau^2 c}{h^2}(u_1 + u_2 - 2u_0) + 2u_0 - u_{\mathrm{I}}$

(II) $c_0 = \frac{\alpha}{\chi_0}c$, $c_1 = c_2 = c$; $\quad u_{\mathrm{II}} = \frac{\tau^2 c}{h^2}\left[\frac{\alpha}{\chi_0}(u_1 + u_2 - 2u_0)\right] + 2u_0 - u_{\mathrm{I}}$

(III) $c_1 = \frac{\alpha}{\chi_1}c$, $c_0 = c_2 = c$; $\quad u_{\mathrm{I}} = \frac{\tau^2 c}{h^2}\left\{\frac{1}{4}\left(\frac{\alpha}{\chi_1} - 1\right)(u_1 - u_2) + (u_1 + u_2 - 2u_0)\right\} + 2u_0 - u_{\mathrm{I}}$

(IV) $c_2 = \frac{\alpha}{\chi_2}c$, $c_0 = c_1 = c$, $\quad u_{\mathrm{I}} = \frac{\tau^2 c}{h^2}\left\{\frac{1}{4}\left(1 - \frac{\alpha}{\chi_2}\right)(u_1 - u_2) + (u_1 + u_2 - 2u_0)\right\} + 2u_0 - u_{\mathrm{I}}$

(V) $c_0 = \frac{\alpha}{\chi_0}c$, $c_1 = \frac{\alpha}{\chi_1}c$, $c_2 = c$; $u_{\mathrm{II}} = \frac{\tau^2 c}{h^2}\left\{\frac{1}{4}\left(\frac{\alpha}{\chi_1} - 1\right)(u_1 - u_2) + \frac{\alpha}{\chi_0}(u_1 + u_2 - 2u_0)\right\} + 2u_0 - u_{\mathrm{I}}$

(VI) $c_0 = \frac{\alpha}{\chi_0}c$, $c_2 = \frac{\alpha}{\chi_2}c$, $c_1 = c$; $u_{\mathrm{II}} = \frac{\tau^2 c}{h^2}\left\{\frac{1}{4}\left(1 - \frac{\alpha}{\chi_2}\right)(u_1 - u_2) + \frac{\alpha}{\chi_0}(u_1 + u_2 - 2u_0)\right\} + 2u_0 - u_{\mathrm{I}}$

(VII) $c_1 = \frac{\alpha}{\chi_1}c$, $c_2 = \frac{\alpha}{\chi_2}c$, $c_0 = c$; $u_{\mathrm{II}} = \frac{\tau^2 c}{h^2}\left\{\frac{\alpha}{4}\left(\frac{1}{\chi_1} - \frac{1}{\chi_2}\right)(u_1 - u_2) + (u_1 + u_2 - 2u_0)\right\} + 2u_0 - u_{\mathrm{I}}$

(VIII) $c_0 = \frac{\alpha}{\chi_0}c$, $c_1 = \frac{\alpha}{\chi_1}c$, $c_2 = \frac{\alpha}{\chi_2}c$; $u_{\mathrm{II}} = \frac{\tau^2 c}{h^2}\left\{\frac{\alpha}{4}\left(\frac{1}{\chi_1} - \frac{1}{\chi_2}\right)(u_1 - u_2) + \frac{\alpha}{\chi_0}(u_1 + u_2 - 2u_0)\right\} + 2u_0 - u_{\mathrm{I}}$

The boundary condition at the top is

$$\frac{\partial u}{\partial x} = 0 \qquad \text{or} \qquad u_1 = u_2 .$$

We can perform the numerical calculation on the vibrations of buildings by making use of the above eight equations step by step.

(ii) Numerical calculations

Taking the height of the building $H = 40$ m, the intervals for finite difference method $h = H/10 = 4m$ and the velocity of equivalent transverse waves of the building $\sqrt{\frac{G}{\rho}} = 320\,m/sec$, the fundamental period of the building in elastic range is $T = 0.50$ sec.

In these calculations, we should consider the most disadvantageous wave attacking the building. Thus assumed earthquake waves were the wave having the alternate constant accerelation with the period 0.50 sec and the sine waves having the periods 0.45, 0.50 and 0.55 sec. The accerelation, velocity and displacement of the former are compared with those of the latter in Fig.28. The maximum amplitude was taken as 5 cm in each case and the time interval of one step of calculation was taken as 0.0125 sec. The transition point from elastic to plastic range was determined by the value of strain α and it was assumed as 0.32 - 0.65. The results of calculations are shown in Fig. 29 -33.

(iii) Consideration

The several examples of numerical calculations, we have made on the vibrations in elastic-plastic range, have led to the following basic considerations.

(1) The displacements due to the plastic strains are generally greater than the displacements due to the elastic strains.

(2) The strains ted to be in plastic near the base, and the regions transit to upward, but in some cases, about midpoint of the height, the strains come into plastic range at first.

(3) The stress distributions in the plastic are more complicated than the distributions in the elastic range, in other words, the former has more unevenness than the latter.

(4) If the structures have plastic regions, the present method of aseismic design using the lateral force coefficient is not sufficient. The response of the building for the most dis advantageous wave of earthquake should be computed also in design, considering the destructive strains in structures instead of the stresses.

5. Conclusion

From some experimental data and numerical calculations developed above, the vibration behavior of special portions of buildings, the variations in earthquake forces due to the ground properties and the vibrations in plastic range were discussed. The discussions of each paragraph suggest the manners of aseismic design in future.

NOMENCLATURE

A : cross-section area of the building

G : modulus of rigidity of the building

ρ : average density of the building

b : width of the building

l , H : height of the building

x : coordinate in the vertical direction

z : coordinate in the horizontal direction

u : horizontal displacement

t : time

n : frequency

T : natural period or kinetic energy

k : coefficient of subgrade reaction

P : external force applied to the building

θ : rotation at the base of the building

I : geometrical moment of inertia

V : potential energy

F : damping energy

w : total displacement in the horizontal direction

r : horizontal displacement due to the rotation

τ_k : shearing stress

τ : time interval or time factor

h : constant spacing of the pivotal points

C : constant or G/ρ

References

1) M.Hatanaka, "On the vibration characteristics of moving coil type vibrograph," Bulletin of the Disaster Prevention Research Inst.,Kyoto University, Memorial Issue of the fifth Anniversary, Nov. 1956, pp.143-152.
2) R.Tanebashi and H.Ishizaki, "Earthquake damages and elastic properties of the ground," Bulletin of the Disaster Prevention Research Inst., Kyoto University, No.4, May 1953.

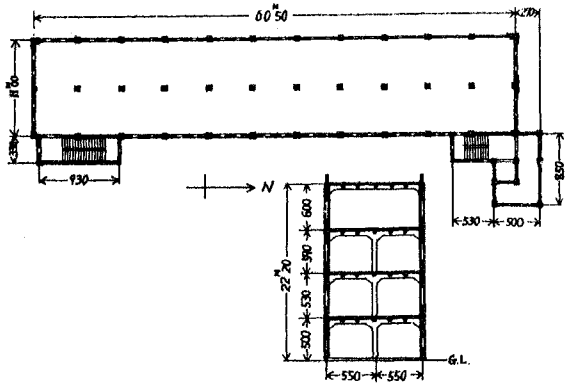

Fig. 1 Plan and section of a four-storied reinforced concrete building.

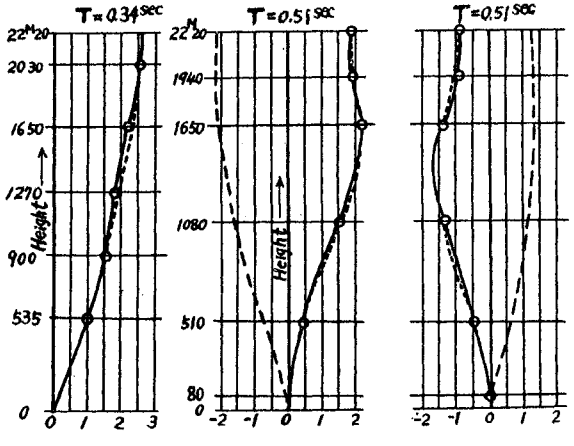

Fig. 2 Typical examples of displacement distributions in vibrations. The dotted lines are obtained by the calculation.

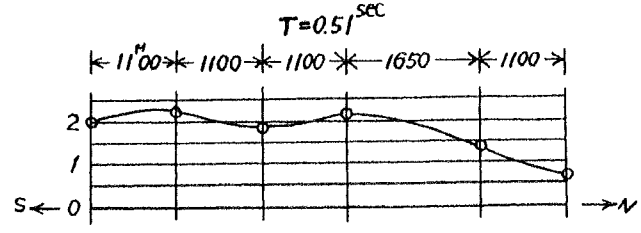

Fig. 3 Displacement distribution in horizontal direction.

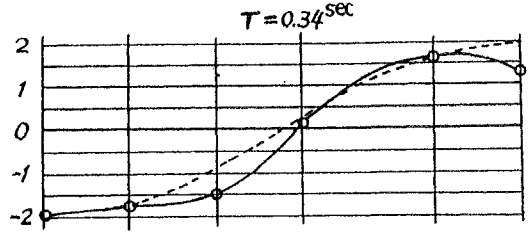

Fig. 4 Displacement distribution in horizontal direction.

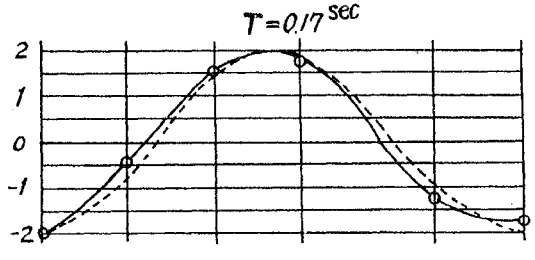

Fig. 5 Displacement distribution in horizontal direction.

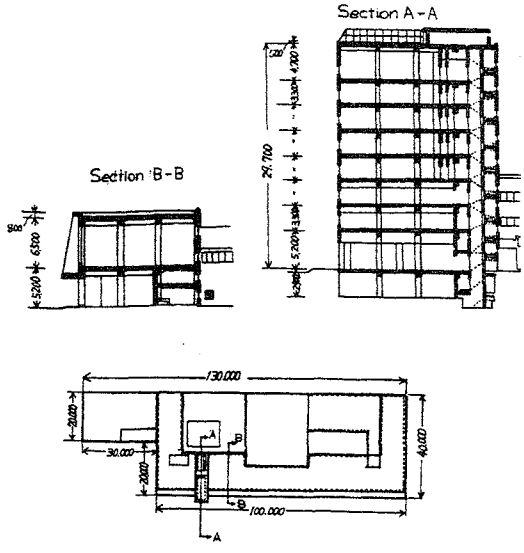

Fig. 6 Plan and sections of Kyoto Station.

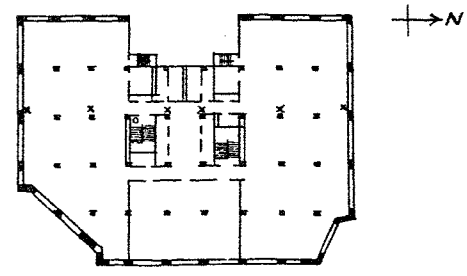

Fig. 8 Plan of a building of 12 stories above and 3 stories under ground.

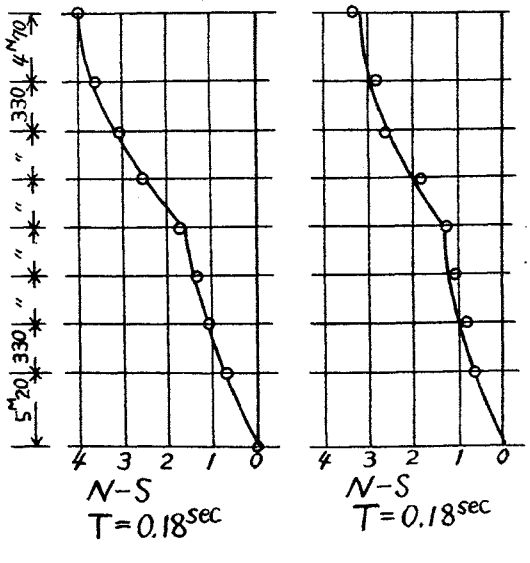

Fig. 7 Examples of displacement distributions in vibrations.

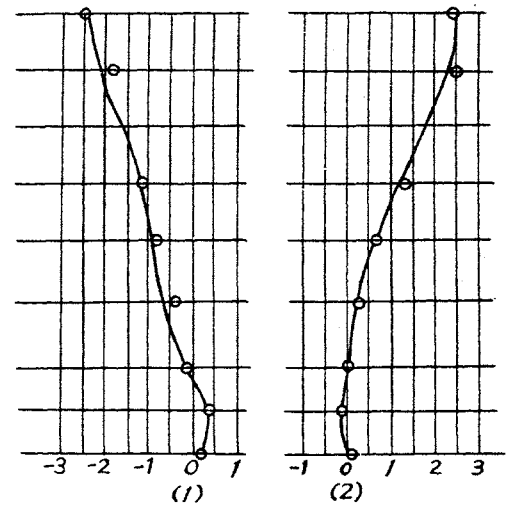

Fig. 9 Displacement distributions in vibrations.

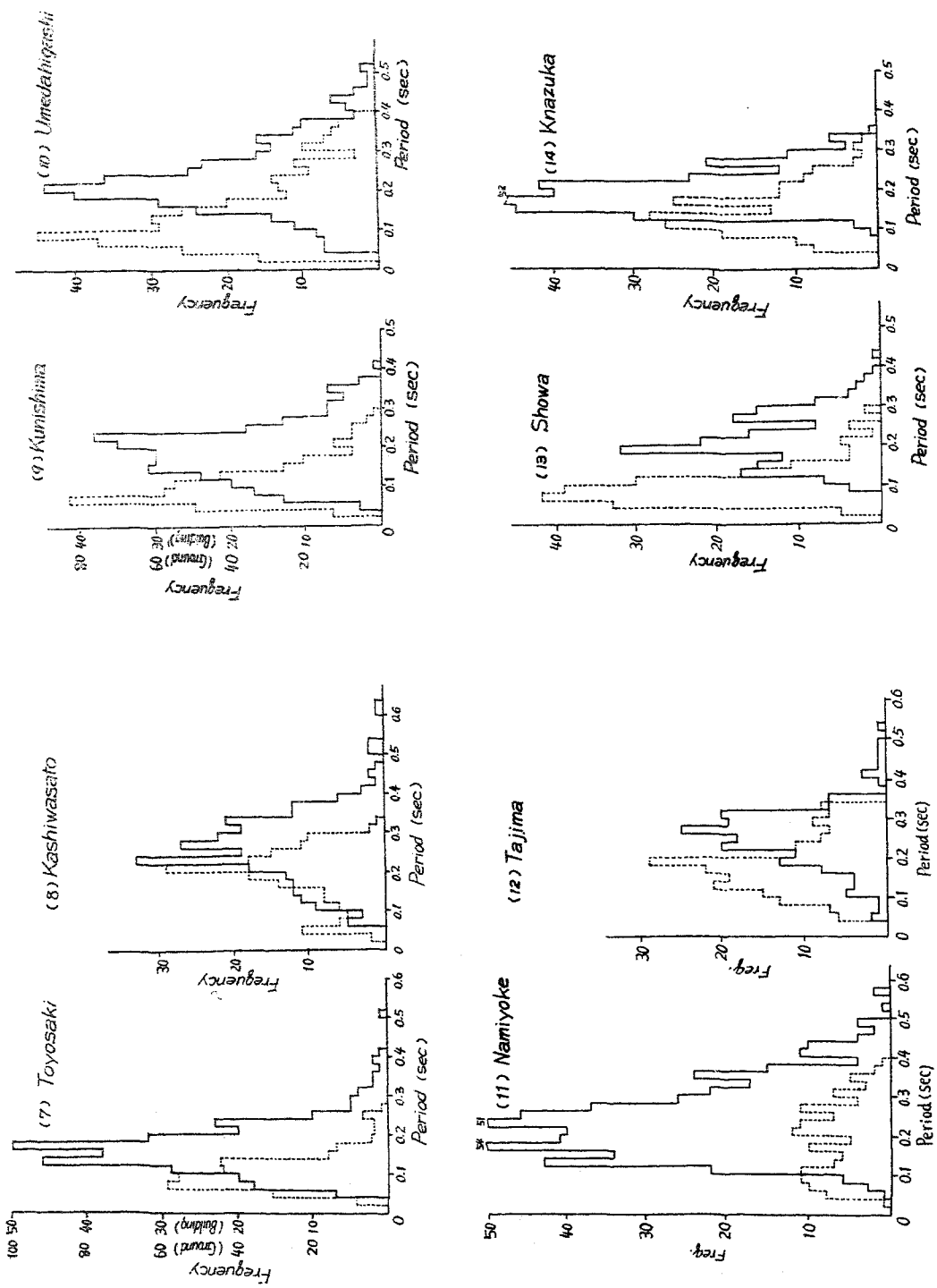

Fig. 15 Examples of frequency distributions of periods.

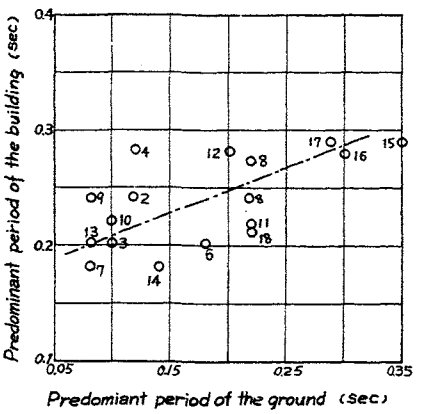

Fig. 16 Relation between predominant period of the building and ground.

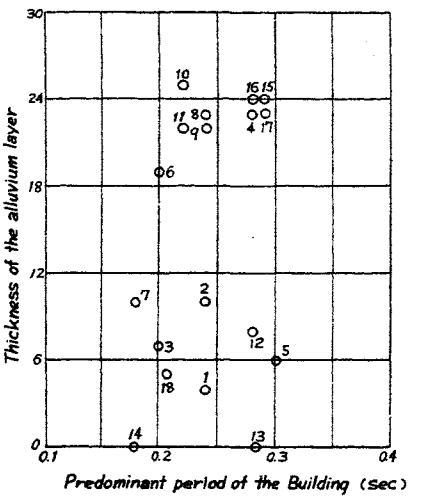

Fig. 17 Relation between predominant period of the building and thickness of the alluvium layer.

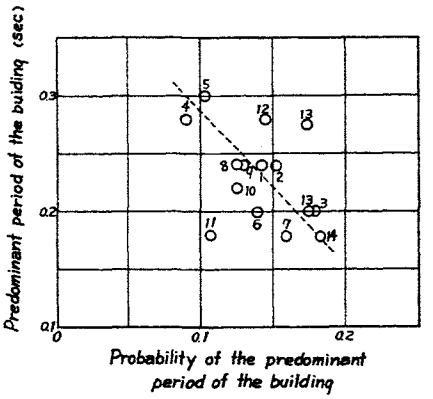

Fig. 18 Relation between predominant period of the building and probability of the predominant period.

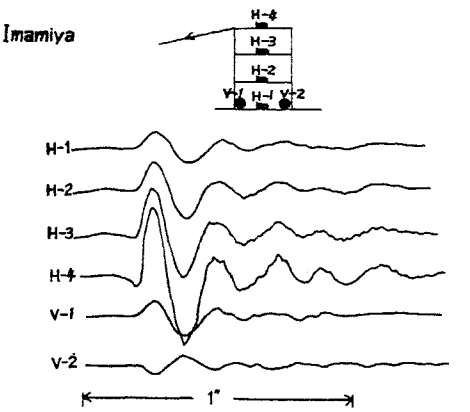

Fig. 20 Example of vibration records.

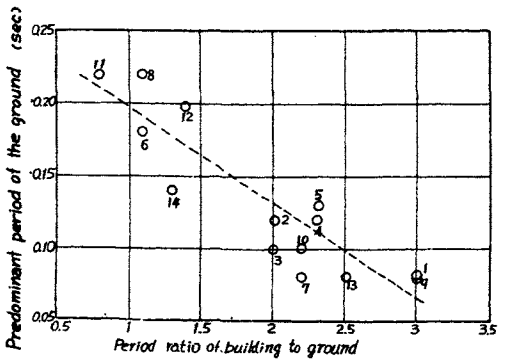

Fig. 19 Relation between predominant period of the building and period ratio of the building to the ground.

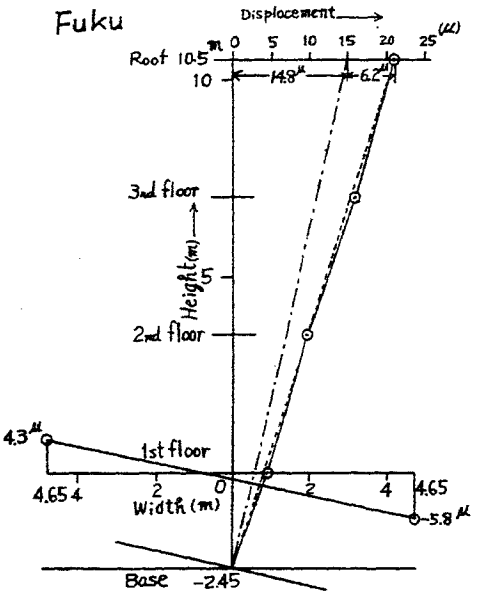

Fig. 21 Displacement distribution (1).

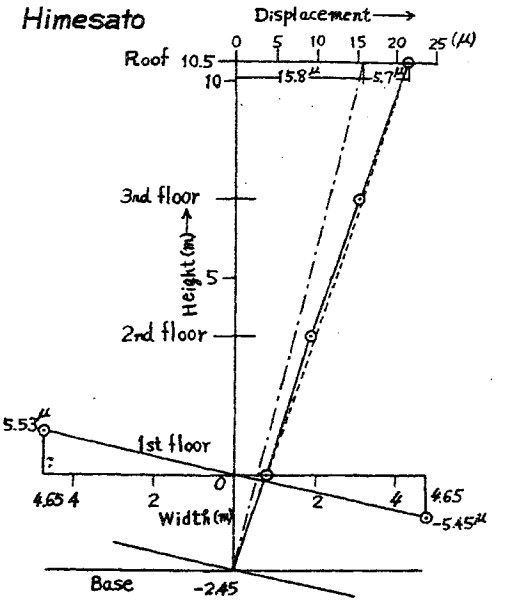

Fig. 22 Displacement distribution (2).

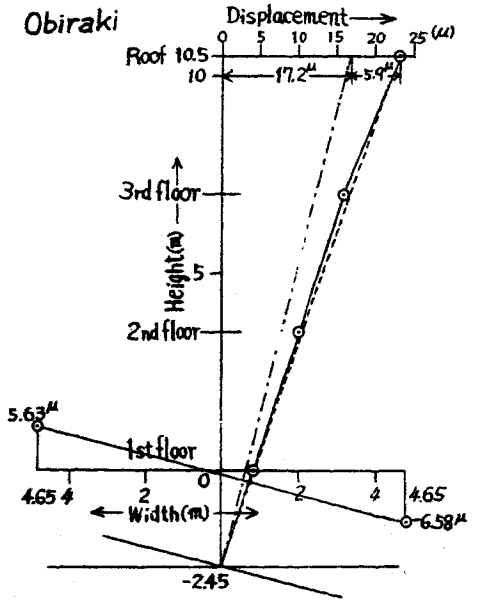

Fig. 23 Displacement distribution (3).

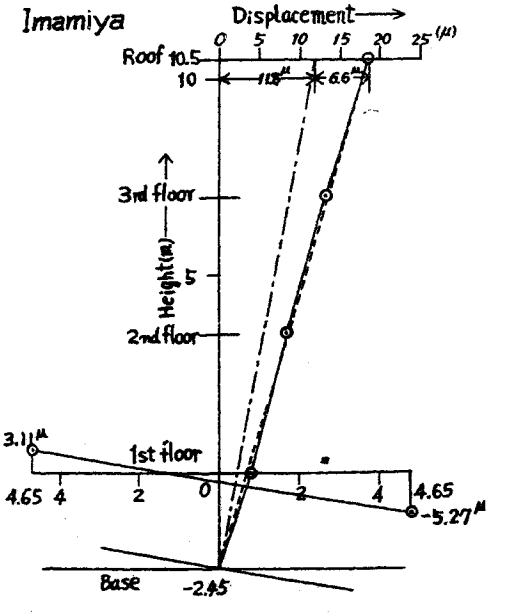

Fig. 24 Displacement distribution (4).

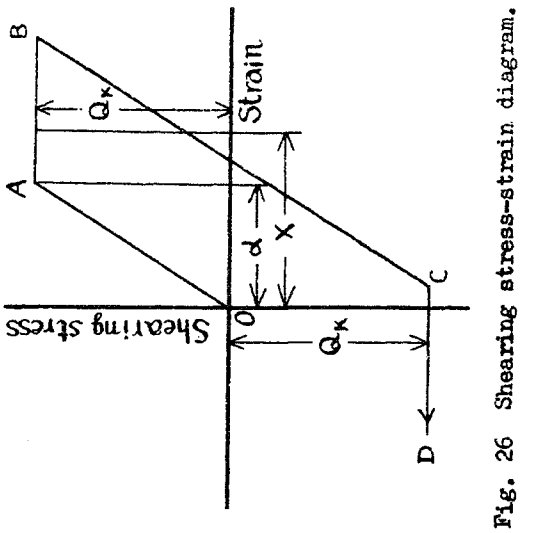

Fig. 26 Shearing stress-strain diagram.

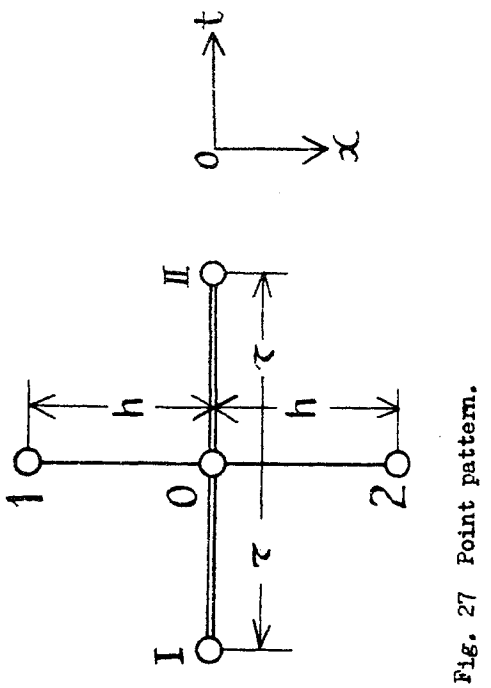

Fig. 27 Point pattern.

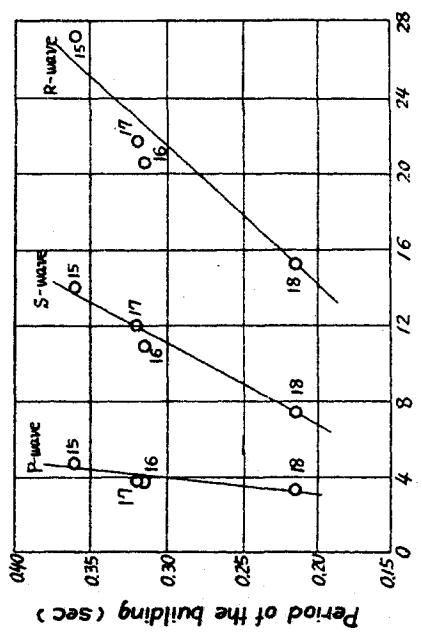

Fig. 25 Relation between period of the building and traveling time of the elastic wave.

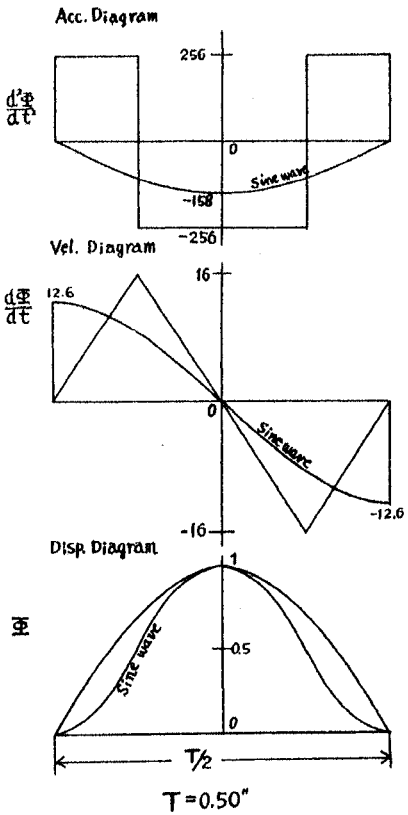

Fig. 28 Accerelations, velocity and displacement diagram of assumed waves.

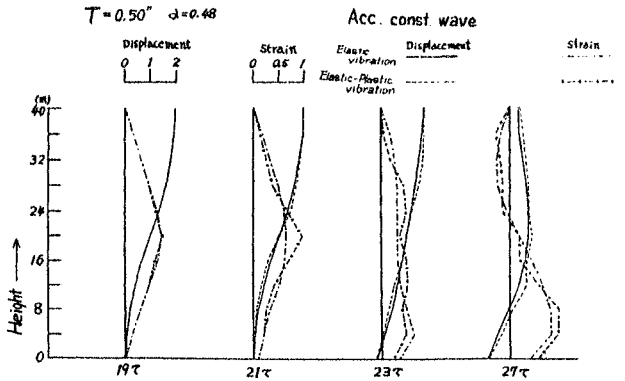

Fig. 29 Displacement and strain distributions in elastic and elastic-plastic vibrations (1).

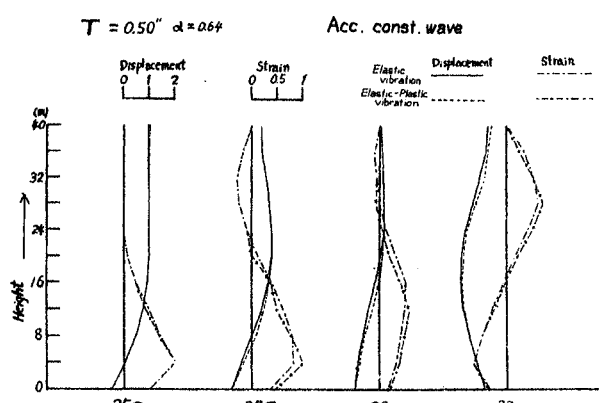

Fig. 30 Displacement and strain distributions in elastic and elastic-plastic vibrations (2).

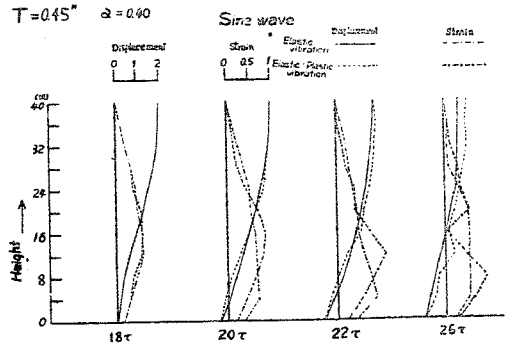

Fig. 31 Displacement and strain distributions in elastic and elastic-plastic vibrations (3).

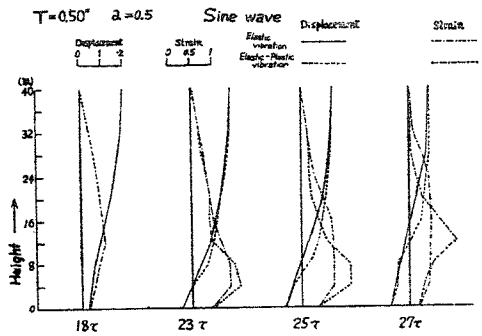

Fig. 32 Displacement and strain distributions in elastic and elastic-plastic vibrations (4).

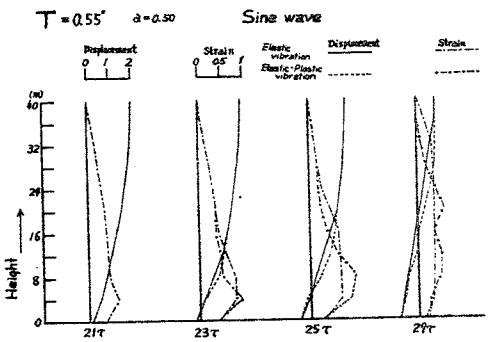

Fig. 33 Displacement and strain distributions in elastic and elastic-plastic vibrations (5).

Table 1

No.	Type of the frequency distribution of period		Predominant period (sec)		Probability of the predominant period		Period ratio	Alluvium thickness (m)
	Building	Ground	Building	Ground	Building	Ground		
1	A	A	0.24	0.08	0.142	0.187	3.0	4
2	A	A-B	0.24	0.12	0.152	0.183	2.0	10
3	A	A	0.20	0.10	0.177	0.165	2.0	7
4	B	C	0.28	0.12	0.089	0.189	2.3	23
5	B	B	0.30	0.13	0.102	0.136	2.3	6
6	B	B	0.20	0.18	0.138	0.149	1.1	19
7	A	A	0.18	0.08	0.158	0.198	2.2	10
8	A-B	A-B	0.24	0.22	0.124	0.178	1.1	23
9	A	A	0.24	0.08	0.128	0.212	3.0	22
10	A	A	0.22	0.10	0.124	0.140	2.2	25
11	C	B	0.18	0.22	0.106	0.083	0.8	22
12	A	A-B	0.28	0.20	0.144	0.150	1.4	8
13	A	B	0.20	0.08	0.173	0.213	2.5	5
14	B	A	0.18	0.14	0.181	0.156	1.3	11
15			0.29					24
16			0.27					24
17			0.29					23
18			0.21					5

Table 2

School	Total deformation ($\times 10^{-3}$mm)	Elastic deformation ($\times 10^{-3}$mm)(u)	Deformation due to the rotation ($\times 10^{-3}$mm)(r)	(r)/(u)
Fuku	21.00	6.2 (29.6%)	14.8 (70.4%)	2.40
Himesato	21.50	5.7 (26.5%)	15.8 (73.5%)	2.77
Obiraki	23.10	5.9 (25.6%)	17.3 (74.4%)	2.91
Imamiya	18.40	6.6 (35.9%)	11.8 (64.1%)	1.79

Table 3

School	Period of the micro-tremor (sec)	Period of the building (sec)
Fuku	0.28 - 0.31	0.35 - 0.37
Himesato	0.26 - 0.29	0.29 - 0.35
Obiraki	0.28 - 0.30	0.31 - 0.32
Imamiya	0.20 - 0.22	0.21 - 0.22

Table 4

School	Rigidity (kg/cm²)	Coefficient of subgrade reaction (kg/cm³)	Computed period (sec)
Fuku	1384	9.98	0.129
Himesato	1517	9.43	0.130
Obiraki	1458	8.62	0.135
Imamiya	1267	12.21	0.122